HE 1166

PERGAMON

International Journal of Hydrogen Energy 000 (2000) 000–000

International Journal of HYDROGEN ENERGY

www.elsevier.com/locate/ijhydene

Observation of extreme ultraviolet emission from hydrogen-KI plasmas produced by a hollow cathode discharge

Randell L. Mills *

BlackLight Power, Inc., 493 Old Trenton Road, Cranbury, NJ 08512, USA

Received 9 August 2000; accepted 24 October 2000

Abstract

A high-voltage discharge of hydrogen with and without the presence of a source of potassium, potassium iodide, in the discharge was performed with a hollow cathode. It has been reported that intense extreme ultraviolet (EUV) emission was observed from atomic hydrogen and certain elements or certain ions which ionize at integer multiples of the potential energy of atomic hydrogen, 27.2 eV (Mills et al., 1999 Pacific Conference on Chemistry and Spectroscopy and the 35th ACS Western Regional Meeting, Ontario Convention Center, California, October 6–8, 1999; Mills et al., Int. J. Hydrogen Energy 25 (2000) 919; Mills, Int. J. Hydrogen Energy, in press; Mills et al., Int. J. Hydrogen Energy, in press; Mills et al., June ACS Meeting, 29th Northeast Regional Meeting, University of Connecticut, Storrs, CT, June 18–21, 2000). Two potassium ions or a potassium atom may each provide an electron ionization or transfer reaction that has a net enthalpy equal to an integer multiple of 27.2 eV. The spectral lines of atomic hydrogen were intense enough to be recorded on photographic films only when KI was present. EUV lines not assignable to potassium, iodine, or hydrogen were observed at 73.0, 132.6, 513.6, 677.8, 885.9, and 1032.9 Å. The lines could be assigned to transitions of atomic hydrogen to lower-energy levels corresponding to lower-energy hydrogen atoms called hydrino atoms and the emission from the excitation of the corresponding hydride ions formed from the hydrino atoms.

1. Introduction

The chemical interaction of potassium with hydrogen at temperatures below 1000 K has shown surprising results in terms of the emission of the Lyman and Balmer lines [1–6] and the formation of novel chemical compounds [1,6–12]. In searching for an explanation of chemical reactions of unusually high energy which produced hydrogen Lyman and Balmer series emission, a resonant electronic interaction between hydrogen and potassium at energy levels of a multiple of the ionization energy of hydrogen, nE_H, has been introduced into the discussion. This hypothesis is supported by the fact that only those elements such as potassium, cesium, and strontium which have bound electrons of energies of $E = nE_H$ show Lyman and Balmer emission during the chemical interaction with atomic hydrogen. Those elements with electronic states of $E \neq nE_H$ show no emission under identical conditions. This paper addresses new electronic energy states of hydrogen. If such states are stable, spectral line emission should be observed in the EUV during their formation and during energetic electron excitation of compounds containing hydrogen in these states.

The following paper reports the first exploratory measurements in the EUV. For this experiment, a standard hollow cathode discharge in hydrogen was employed to generate atomic hydrogen and to provide the energetic electrons. This papers presents the experimental results and compares it with theoretical considerations.

A historical motivation to cause EUV emission from a hydrogen gas was that the spectrum of hydrogen was first recorded from the only known source, the Sun [13]. Developed sources that provide a suitable intensity are high-voltage discharge and inductively coupled plasma generators [14]. An important variant of the later type of source is a tokomak [15]. Fujimoto et al. [16] have determined the cross section for production of excited hydrogen atoms from the emission cross sections for Lyman and

* Tel.: +1-609-490-1040; fax: +1-609-490-1066.
E-mail address: rmills@blacklightpower.com (R.L. Mills).

0360-3199/01/$20.00
PII: S0360-3199(00)00122-1

Balmer lines when molecular hydrogen is dissociated into excited atoms by electron collisions. This data was used to develop a collisional-radiative model to be used in determining the ratio of molecular-to-atomic hydrogen densities in tokomak plasmas. Their results indicate an excitation threshold of 17 eV for Lyman α emission. Addition of other gases would be expected to decrease the intensity of hydrogen lines which could be absorbed by the gas. Hollander and Wertheimer [17] found that within a selected range of parameters of a plasma created in a microwave resonator cavity, a hydrogen–oxygen plasma displays an emission that resembles the absorption of molecular oxygen. Whereas, a helium–hydrogen plasma emits a very intense hydrogen Lyman α radiation at 121.5 nm which is up to 40 times more intense than other lines in the spectrum. The Lyman α emission intensity showed a significant deviation from that predicted by the model of Fujimoto et al. [16] and from the emission of hydrogen alone.

It has been reported [1–6] that EUV emission of atomic and molecular hydrogen occurs in the gas phase at low temperatures (e.g. $< 10^3$ K) upon contact of atomic hydrogen with certain vaporized elements or ions. Atomic hydrogen was generated by dissociation at a tungsten filament and at a transition metal dissociator that was incandescently heated by the filament. Various elements or ions were made gaseous by heating to form a low vapor pressure (e.g. 1 Torr). The kinetic energy of the thermal electrons at the experimental temperature of $< 10^3$ K were about 0.1 eV, and the average collisional energies of electrons accelerated by the field of the filament were less than 1 eV. (No blackbody emission was recorded for wavelengths shorter than 400 nm.) Atoms or ions which ionize at integer multiples of the potential energy of atomic hydrogen (e.g. cesium, potassium, strontium, and Rb^+) caused hydrogen EUV emission whereas, other chemically equivalent or similar atoms (e.g. sodium, magnesium, holmium, and zinc metals) caused no emission. Helium ions present in the experiment of Hollander and Wertheimer [17] ionize at a multiple of two times the potential energy of atomic hydrogen. The mechanism of EUV emission cannot be explained by the conventional chemistry of hydrogen, but it is predicted by a solution of the Schrodinger equation with a nonradiative boundary constraint put forward by Mills [1–6].

Mills predicts that certain atoms or ions serve as catalysts to release energy from hydrogen to produce an increased binding energy hydrogen atom called a *hydrino atom* having a binding energy of

$$\text{Binding energy} = \frac{13.6\ \text{eV}}{n^2}, \tag{1}$$

where

$$n = \frac{1}{2}, \frac{1}{3}, \frac{1}{4}, \ldots, \frac{1}{p} \tag{2}$$

and p is an integer greater than 1, designated as $H[a_H/p]$ where a_H is the radius of the hydrogen atom. Hydrinos are predicted to form by reacting an ordinary hydrogen atom with a catalyst having a net enthalpy of reaction of about

$$m \times 27.2\ \text{eV} \tag{3}$$

where m is an integer. This catalysis releases energy from the hydrogen atom with a commensurate decrease in size of the hydrogen atom, $r_n = na_H$. For example, the catalysis of $H(n=1)$ to $H(n=1/2)$ releases 40.8 eV, and the hydrogen radius decreases from a_H to $\frac{1}{2}a_H$.

The excited energy states of atomic hydrogen are also given by Eq. (1) except that

$$n = 1, 2, 3, \ldots . \tag{4}$$

The $n = 1$ state is the "ground" state for "pure" photon transitions (the $n = 1$ state can absorb a photon and go to an excited electronic state, but it cannot release a photon and go to a lower-energy electronic state).

However, an electron transition from the ground state to a lower-energy state is possible by a nonradiative energy transfer such as multipole coupling or a resonant collision mechanism. These lower-energy states have fractional quantum numbers, $n = 1/\text{integer}$. Processes that occur without photons and that require collisions are common. For example, the exothermic chemical reaction of $H + H$ to form H_2 does not occur with the emission of a photon. Rather, the reaction requires a collision with a third body, M, to remove the bond energy: $H + H + M \rightarrow H_2 + M^*$ [19]. The third body distributes the energy from the exothermic reaction, and the end result is the H_2 molecule and an increase in the temperature of the system. Some commercial phosphors are based on nonradiative energy transfer involving multipole coupling. For example, the strong absorption strength of Sb^{3+} ions along with the efficient nonradiative transfer of excitation from Sb^{3+} to Mn^{2+}, are responsible for the strong manganese luminescence from phosphors containing these ions [20]. Similarly, the $n = 1$ state of hydrogen and the $n = 1/\text{integer}$ states of hydrogen are nonradiative, but a transition between two nonradiative states is possible via a nonradiative energy transfer, say $n = 1$ to $1/2$. In these cases, during the transition the electron couples to another electron transition, electron transfer reaction, or inelastic scattering reaction which can absorb the exact amount of energy that must be removed from the hydrogen atom. Thus, a catalyst provides a net positive enthalpy of reaction of $m \times 27.2$ eV (i.e. it absorbs $m \times 27.2$ eV where m is an integer). Certain atoms or ions serve as catalysts which resonantly accept energy from hydrogen atoms and release the energy to the surroundings to effect electronic transitions to fractional quantum energy levels given by Eqs. (1) and (2).

2. Inorganic catalysts

A catalytic system is provided by the ionization of t electrons from an atom to a continuum energy level such that the sum of the ionization energies of the t electrons is

approximately $m \times 27.2$ eV where m is an integer. One such catalytic system involves potassium. The first, second, and third ionization energies of potassium are 4.34066, 31.63, 45.806 eV, respectively [21]. The triple ionization ($t = 3$) reaction of K to K^{3+}, then, has a net enthalpy of reaction of 81.7426 eV, which is equivalent to $m = 3$ in Eq. (3):

$$81.7426 \text{ eV} + \text{K}(m) + \text{H}\left[\frac{a_H}{p}\right] \rightarrow \text{K}^{3+} + 3\text{e}^- + \text{H}\left[\frac{a_H}{(p+3)}\right] + [(p+3)^2 - p^2] \times 13.6 \text{ eV}, \quad (5)$$

$$\text{K}^{3+} + 3\text{e}^- \rightarrow \text{K}(m) + 81.7426 \text{ eV} \quad (6)$$

and, the overall reaction is

$$\text{H}\left[\frac{a_H}{p}\right] \rightarrow \text{H}\left[\frac{a_H}{(p+3)}\right] + [(p+3)^2 - p^2] \times 13.6 \text{ eV}. \quad (7)$$

Potassium ions can also provide a net enthalpy of a multiple of that of the potential energy of the hydrogen atom. The second ionization energy of potassium is 31.63 eV; and K^+ releases 4.34 eV when it is reduced to K. The combination of reactions K^+ to K^{2+} and K^+ to K, then, has a net enthalpy of reaction of 27.28 eV, which is equivalent to $m = 1$ in Eq. (3):

$$27.28 \text{ eV} + \text{K}^+ + \text{K}^+ + \text{H}\left[\frac{a_H}{p}\right] \rightarrow \text{K} + \text{K}^{2+} + \text{H}\left[\frac{a_H}{(p+1)}\right] + [(p+1)^2 - p^2] \times 13.6 \text{ eV}, \quad (8)$$

$$\text{K} + \text{K}^{2+} \rightarrow \text{K}^+ + \text{K}^+ + 27.28 \text{ eV}.$$

The overall reaction is

$$\text{H}\left[\frac{a_H}{p}\right] \rightarrow \text{H}\left[\frac{a_H}{(p+1)}\right] + [(p+1)^2 - p^2] \times 13.6 \text{ eV} \quad (10)$$

3. Hydrino catalysts

Lower-energy hydrogen atoms, *hydrinos*, can act as catalysts because each of the metastable excitation, resonance excitation, and ionization energy of a hydrino atom is $m \times 27.2$ eV (Eq. (2)). The transition reaction mechanism of a first hydrino atom affected by a second hydrino atom involves the resonant coupling between the atoms of m degenerate multipoles each having 27.21 eV of potential energy [18]. The energy transfer of $m \times 27.2$ eV from the first hydrino atom to the second hydrino atom causes the central field of the first atom to increase by m and its electron to drop m levels lower from a radius of a_H/p to a radius of $a_H/(p+m)$. The second interacting lower-energy hydrogen is either excited to a metastable state, excited to a resonance state, or ionized by the resonant energy transfer. The resonant transfer may occur in multiple stages. For example, a nonradiative transfer by multipole coupling may occur wherein the central field of the first increases by m, then the electron of the first drops m levels lower from a radius of a_H/p to a radius of $a_H/(p+m)$ with further resonant energy transfer. The energy transferred by multipole coupling may occur by a mechanism that is analogous to photon absorption involving an excitation to a virtual level. Or, the energy transferred by multipole coupling and during the electron transition of the first hydrino atom may occur by a mechanism that is analogous to two photon absorption involving a first excitation to a virtual level and a second excitation to a resonant or continuum level [22–24]. The transition energy greater than the energy transferred to the second hydrino atom may appear as a photon in a vacuum medium.

For example, the transition of $H[a_H/p]$ to $H[a_H/(p+m)]$ induced by a resonance transfer of $m \times 27.21$ eV (Eq. (3)) with a metastable state excited in $H[a_H/p']$ is represented by

$$m \times 27.2 \text{ eV} + \text{H}\left[\frac{a_H}{p'}\right] + \text{H}\left[\frac{a_H}{p}\right] \rightarrow \text{H}\left[\frac{a_H}{p'}\right] + \text{H}\left[\frac{a_H}{p+m}\right] + [(p+m)^2 - p^2] \times 13.6 \text{ eV}, \quad (11)$$

$$\text{H}^*\left[\frac{a_H}{p}\right] \rightarrow \text{H}\left[\frac{a_H}{p'}\right] + m \times 27.2 \text{ eV}. \quad (12)$$

And, the overall reaction is

$$\text{H}\left[\frac{a_H}{p}\right] \rightarrow \text{H}\left[\frac{a_H}{p+m}\right] + [(p+m)^2 - p^2] \times 13.6 \text{ eV}, \quad (13)$$

where p, p', and m are integers and the asterisk represents an excited metastable state.

The transition of $H[a_H/p]$ to $H[a_H/(p+m)]$ induced by a multipole resonance transfer of $m \times 27.21$ eV (Eq. (3)) and a transfer of $[(p')^2 - (p'-m')^2] \times 13.6 \text{ eV} - m \times 27.2$ eV with a resonance state of $H[a_H/(p'-m')]$ excited in $H[a_H/p']$ is represented by

$$\text{H}\left[\frac{a_H}{p'}\right] + \text{H}\left[\frac{a_H}{p}\right] \rightarrow \text{H}\left[\frac{a_H}{p'-m'}\right] + \text{H}\left[\frac{a_H}{p+m}\right] + [((p+m)^2 - p^2) - (p'^2 - (p'-m')^2)] \times 13.6 \text{ eV}, \quad (14)$$

where p, p', m, and m' are integers.

3.1. Hydride ions

A novel hydride ion having extraordinary chemical properties given by Mills [18] is predicted to form by the reaction

Table 1
The ionization energy of the hydrino hydride ion $H^-(n = 1/p)$ as a function of p

Hydride ion	r_1 (a_0)[a]	Calculated ionization energy[b] (eV)	Calculated wavelength (Å)
$H^-(n = 1/2)$	0.9330	3.047	4070
$H^-(n = 1/3)$	0.6220	6.610	1880
$H^-(n = 1/4)$	0.4665	11.23	1100
$H^-(n = 1/5)$	0.3732	16.70	742
$H^-(n = 1/6)$	0.3110	22.81	544

[a]From Eq. (17).
[b]From Eq. (16).

of an electron with a hydrino (Eq. (15)). The resulting hydride ion is referred to as a hydrino hydride ion, designated as $H^-(1/p)$:

$$H\left[\frac{a_H}{p}\right] + e^- \rightarrow H^-(1/p). \quad (15)$$

The hydrino hydride ion is distinguished from an ordinary hydride ion having a binding energy of 0.8 eV. The latter is hereafter referred to as "ordinary hydride ion". The hydrino hydride ion is predicted [18] to comprise a hydrogen nucleus and two indistinguishable electrons at a binding energy according to the following formula:

$$\text{Binding energy} = \frac{\hbar^2\sqrt{s(s+1)}}{8\mu_e a_0^2[(1+\sqrt{s(s+1)})/p]^2} - \frac{\pi\mu_0 e^2\hbar^2}{m_e^2 a_0^3}\left(1 + \frac{2^2}{[(1+\sqrt{s(s+1)})/p]^3}\right), \quad (16)$$

where p is an integer greater than one, $s = 1/2$, π is pi, $\hbar$ is Planck's constant bar, μ_0 is the permeability of vacuum, m_e is the mass of the electron, μ_e is the reduced electron mass, a_0 is the Bohr radius, and e is the elementary charge. The ionic radius is

$$r_1 = \frac{a_0}{p}(1 + \sqrt{s(s+1)}), \quad s = \frac{1}{2}. \quad (17)$$

From Eq. (17), the radius of the hydrino hydride ion $H^-(1/p)$; p = integer is $1/p$ times that of ordinary hydride ion, $H^-(1/1)$. The predicted binding energies and ionic radii for the first five hydrino hydride ions are given in Table 1.

INP Greifswald, Germany recorded spectra of a hollow cathode plasma source in the range of 2.5–80 nm at the request of BlackLight Power, Inc. of Cranbury, NJ, USA [25]. This plasma source, called a BLP-source, consisted of a five-way cross containing a hollow cathode discharge tube and a heated pipe comprising a reservoir for vaporizing KI. One end of the reservoir was closed, and the other open end was mounted close to the exit of the hollow cathode. The axis of both cylindrical pieces, the hollow cathode and the heated reservoir, were arranged almost perpendicular to each other.

A 4° grazing incidence spectrometer was attached to the BLP-source. At this shallow angle of incidence, a strong astigmatism stretches each point like a divergent light source at the entrance slit into a line in the focal plane. The spectrometer was filled with hydrogen during operation via the BLP source. Due to differential pumping a pressure drop was established between the source and the spectrometer.

The proper functioning of the spectrometer in the desired wavelengths range was demonstrated by using a known capillary discharge in high vacuum that emitted carbon and oxygen spectra of multiply ionized atoms down to 3.5 nm.

Potassium iodide was used as a source of potassium. Based on its reported exceptional emission [1–4,6], potassium was a good choice for a catalyst according to Eqs. (5)–(7) to cause transitions in hydrogen to lower energy levels to form hydrino atoms. The hydrino atoms then also served as catalysts according to Eqs. (11)–(13) and (14). Hydrino hydride ions formed by the reaction of plasma electrons with hydrino atoms. Compounds containing hydrino hydride ions were observed by their characteristic emission when excited in the plasma discharge.

4. Methods

4.1. Standard hydrogen emission spectrum

A standard atomic and molecular hydrogen extreme ultraviolet emission spectrum was obtained by BlackLight Power, Inc., Cranbury, NJ with a microwave discharge system and an EUV spectrometer. The microwave generator was a Opthos model MPG-4M generator (Frequency: 2450 MHz). The output power was set at 85 W. Hydrogen gas was flowed through a half-inch diameter quartz tube at 550 mTorr. The tube was fitted with an Opthos coaxial microwave cavity (Evenson cavity). The EUV spectrometer was a McPherson model 302 (Seya-Namioka type) normal incidence monochromator. The monochromator slits was 30 × 30 μm. A sodium salicylate converter was used, and the emission was detected with a photomultiplier tube detector (Hamamatsu R1527P).

4.2. Capillary discharge

A certain discharge type has become very important for a couple of special applications. For example, in the field of radiation generation in the EUV or soft X-ray region the so-called capillary discharge is often used [26]. Several scientists have shown that it is possible to generate laser radiation at shorter wavelengths by means of a capillary discharge because fast capillary discharges with a large length-to-diameter ratio can generate highly ionized plasmas. The field is quite advanced [27,28] to the point that Rocca [27] has developed a table top laser using the 46.9 nm Argon line.

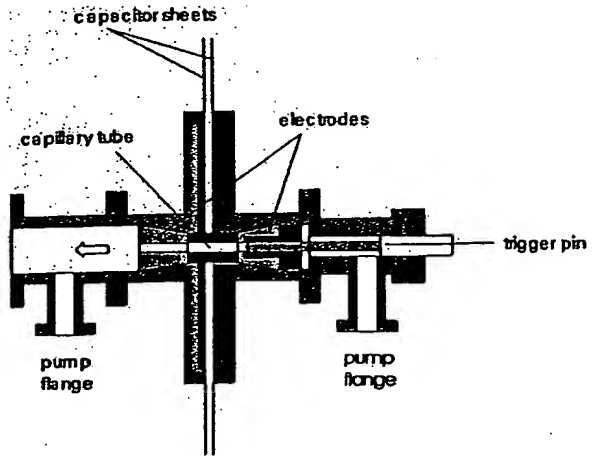

Fig. 1. Capillary discharge vessel.

A high electric power is required to excite atoms to high electronic energy levels. Since a high-energy input into a device is unwanted, a technically convenient energy has to be delivered to a plasma in a short time. The capillary discharge described by Bogen et al. [26] has an electric current rise time and an emission time of the hydrogen like carbon VII line that is shorter than 50 ns.

A cross-sectional view of the capillary discharge system is shown in Fig. 1. The capacitor, leads, capillary for plasma production, switch, and trigger were all integrated in a single unit in order to maintain a low inductance. The capacitor was a copper laminated plastic sheet with isolation gaps along the rim and in the center. A plastic disk with a plastic cylinder in the center provided additional high-voltage insulation. The plastic cylinder penetrated the capacitor and was encapsulated on each end by brass pieces. Hollow carbon electrodes were attached at each end of the plastic cylinder by the brass pieces which pressed the electrodes. The brass pieces were soldered to the copper laminate of the capacitor. The plastic cylinder and the carbon electrodes had a common borehole along the axis of the cylinder.

The plasma was observed end on from one side. On the other side, a carbon trigger pin provided a spark when a sharply rising potential was applied between this trigger pin and one of the carbon electrodes. This spark triggered the discharge of the capacitor. A plasma was formed inside the plastic cylinder borehole which comprised the capillary. This plasma had an electron temperature of up to 50 eV and an electron density of up to 10^{25} particles per m^3 [29]. The brass pieces were connected to a vacuum system. This arrangement permitted the end-on observation of the generated spark. To avoid a pressure gradient, the trigger side of the discharge as well as the spectrograph side were evacuated by a pumping system shown in Fig. 1.

Table 2
Parameters used in the capillary discharge experiments

Discharge voltage V	6–10 kV
Discharge pressure p	$\leqslant 10^{-5}$ mbar
Capacitor capacitance C	19 nF
Capacitor inductance I	19 nH
Thickness of the Makrolon foil b	200 nm
Number of single discharges n	About 500

4.3. System for EUV measurement of discharge

In order to protect the electronic devices from destruction and to avoid disturbances while measuring, the discharge source, the entire power supply, and the pumping system was placed in a grounded Faraday cage. The capacitor was charged via 1 MΩ resistor. The discharge was driven by a power supply in a voltage range between 6 and 10 kV. In addition, a second power supply was used to provide a very fast high-voltage pulse (4 kV with a rise time of 10 ns) to the trigger pin. This pulse provided a controlled ignition of the capillary discharge.

For more convenient operation, the EUV-spectrograph was located outside of the Faraday cage. In a capillary discharge, a spectrum is generated by excitation of atoms of an evaporated dielectric material. Polyethylene (PE) or polyacetal (PA) was used in the present study. The discharge produced a lot of dust. Therefore, a special Makrolon foil (polycarbonate) with a thickness of about 200 nm that was transparent to the soft X-ray and EUV region light of this study [] was placed between the capillary discharge and the EUV-spectrograph to protect the grating. The spectrograph as well as the whole discharge vessel were connected with the pumping system. The discharge was driven in vacuum at a working pressure of 10^{-5} mbar or less. For time-resolved measurements, the spectrograph was replaced by a fast photo multiplier that permitted examination of the temporal behavior of a single spark. Table 2 gives the main parameters of this experiment. The experimental setup is shown in Fig. 2.

4.4. EUV-spectrograph and photochemical detector

The spectrometer was a LSP-VUV 1-3S-M portable EUV grazing incidence spectrometer that used an off Rowland circle registration scheme wherein the diameter of the Rowland circle corresponded to the radius of curvature of the grating. In this study, the spectra were recorded in a single plane. Thus, the input slit was focused only for a single wavelength (center wavelength λ_0). The alignment to a different wavelength was produced by simply changing the distance between the focal plane and the grating. The spectra were detected using a special Russian EUV film.

The grazing angle of incidence to the grating was rated by the manufacturer to be 4°. The width of the entrance slit was chosen to be 100 μm. The spectral resolution $\lambda/\Delta\lambda$ was better than 100. The grating parameters are shown in

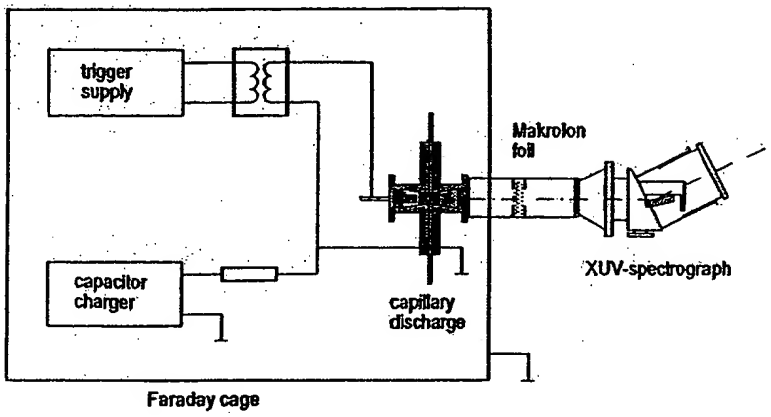

Fig. 2. Experimental setup for capillary discharge measurements.

Table 3
Grating parameters

Radius of curvature (mm)	1000		
Size of ruled area (mm)	28 × 30		
Coating	Au 300 Å		
Number of grooves (mm)	1200	600	300
Blaze angle (deg)	1		3
Recommended spectral range (Å)	25–60	60–120	120–800

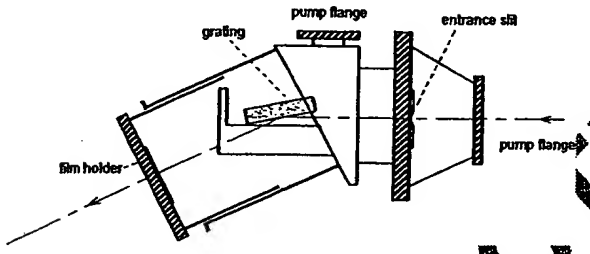

Fig. 3. Cross sectional view of the LSP-VUV-3S-M portable EUV grazing incidence spectrometer.

Table 3. The cross sectional view of the EUV spectrometer is shown in Fig. 3.

4.5. Measurements

The main purpose for the use of a capillary discharge was to demonstrate the spectral range over which the system was capable of recording. The EUV spectrum of a capillary discharge of a polyacetal capillary tube was obtained with the results given shown in Fig. 4 and in Table 4. The numbered spectral lines (with respect to Fig. 4) are assigned to the corresponding wavelengths and energy levels. For an appropriate assignment, it was necessary to calculate the transformation from the plane of registration to the Rowland circle using the specific dispersion function of the grating. Emission could be observed down to 7 nm.

4.6. Experimental setup of the BLP source

The emission of the BLP source (BlackLight Power, Inc., Cranbury, NJ) was investigated in the EUV and soft X-ray region. The plasma cell comprised a five-way stainless-steel cross. The plasma was generated at a hollow cathode inside the discharge cell. The hollow cathode was constructed of a stainless-steel rod inserted into a steel tube, and this assembly was inserted into an alumina tube. A flange opposite the end of the hollow cathode connected the spectrometer with the cell. It had a small hole that permitted radiation to pass to the spectrometer. In addition, a quartz tube positioned perpendicularly to the hollow cathode was attached to two copper high-voltage feedthroughs by means of a tungsten filament. The quartz tube served as a catalyst reservoir when filled with KI.

The electrical copper feedthroughs were connected to a power supply (U = 0–6.3 V, I = 0–40 A) to power the tungsten filament to heat the catalyst in the quartz tube. Some of the KI was observed to vaporize when the filament glowed orange. Another power supply (U=0–20 kV, I=0–30 mA) was connected to the hollow cathode to generate a discharge. A Swagelok adapter at the very end of the steel cross provided a gas inlet and a connection with the pumping system. A diagram of the BLP plasma source is given in Fig. 5.

A high-speed shutter placed between the discharge cell and the spectrograph allowed for control of the detector

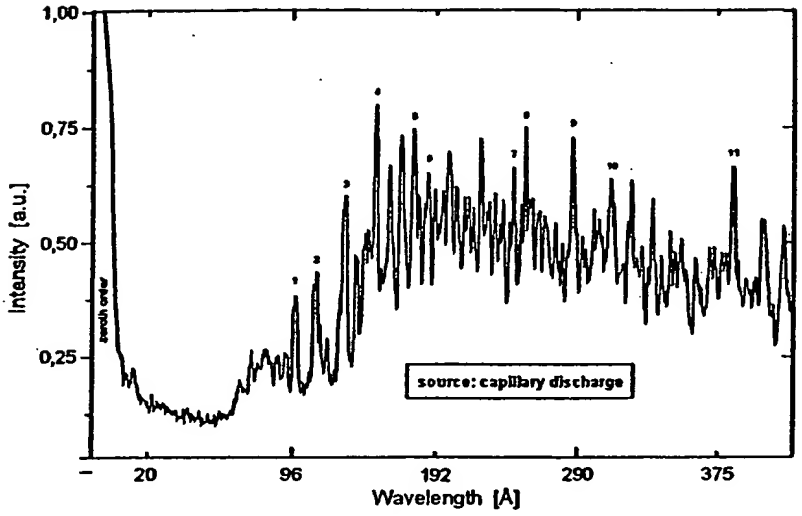

Fig. 4. Spectrum of a capillary discharge.

Table 4
Spectral lines of Fig. 4 with corresponding transitions and wavelengths

Number	Ion	Energy level	Wavelength (Å)
1	O VII	1s2p–1s4d	96.1
2	O VI	$1s^22p$–1s	110
3	O VI	$1s^22p$–1s	130
4	O VI	$1s^22p$–1s	150
5	O VI	1s–$1s^23d$	173
6	O VI	$1s^22p$–$1s^23s$	184
7	C IV	$1s^22p$–$1s^26d$	245
8	C IV	1s2p–$1s^25d$	259
9	C IV	$1s^22p$–$1s^24d$	289
10	C IV	$1s^22p$–$1s^23p$	312
11	C IV	$1s^22p$–$1s^23d$	384

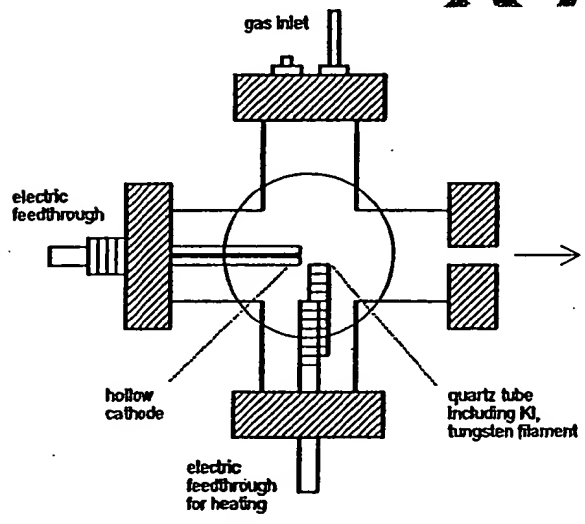

Fig. 5. Cross sectional view of the BLP discharge cell.

exposure time (see EUV-Spectrograph and Photochemical Detector Section). The hollow cathode, shutter, and EUV spectrograph were aligned on a common optical axis using a laser. The experimental setup for the BLP discharge measurements is illustrated in Fig. 6.

4.7. Measurements on the BLP source

The temperature of the tungsten filament which heated the quartz tube was determined by means of a special infrared camera system made by Jenoptic. The evaluation photos showed that the filament had a temperature of at least 1000 K, and the quartz tube was about 80 K colder. The temperature of 920 K was sufficient to melt and vaporize KI in the pressure range of the experiment.

The EUV emission spectrum of the BLP source was obtained during a plasma discharge in hydrogen with and without KI catalyst. Manipulated experimental parameters included the pressure, the temperature and position of the

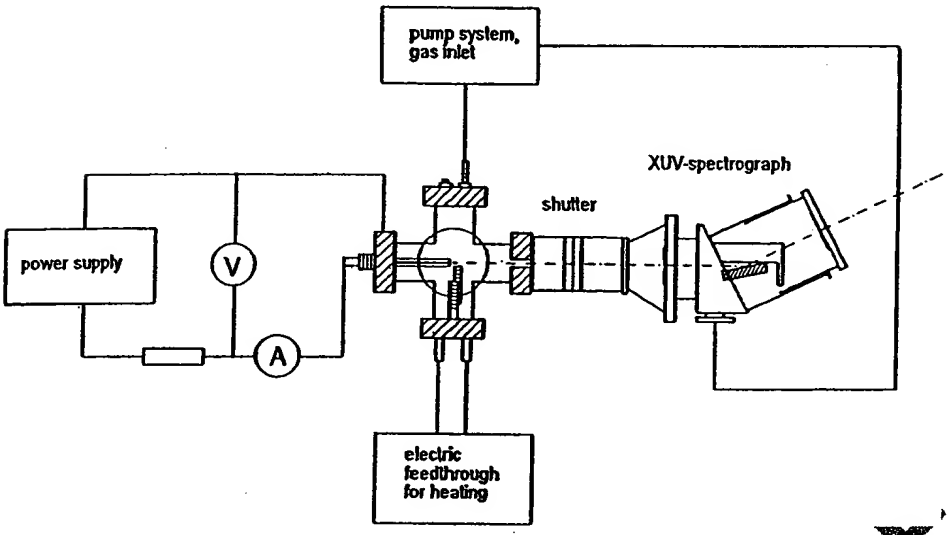

Fig. 6. Experimental setup for the BLP discharge measurements.

catalyst reservoir, the discharge voltage and current, the time of exposure of the detector film system, the particular grating, and the center wavelength λ_0. The main parameter changes and basic spectrographic findings, are presented.

In order to make the wavelength assignments, all of the films were scanned, and the bitmap files were read out as shown in Fig. 4 for the case of the capillary discharge. The measured and calculated spectral lines were numbered from 1 (inside order) to 23. Corresponding lines of different films were assigned the same number based on the specific distances between the grating and the plane of the film that was a function of λ_0. A first wavelength assignment was performed by calculating the transformation from the plane of registration to the Rowland circle using the specific dispersion function of the particular grating.

A number of experiments proved that line No. 12 was the Lyman alpha line with a known wavelength of 1215.7 Å. This wavelength was used to determine the experimental angle of incidence. Thus, a slight divergence to the experiment was detected ($\Delta\angle = 0.33°$), and the dispersion function was recalculated using the experimentally determined angle of grazing incidence of [illegible].

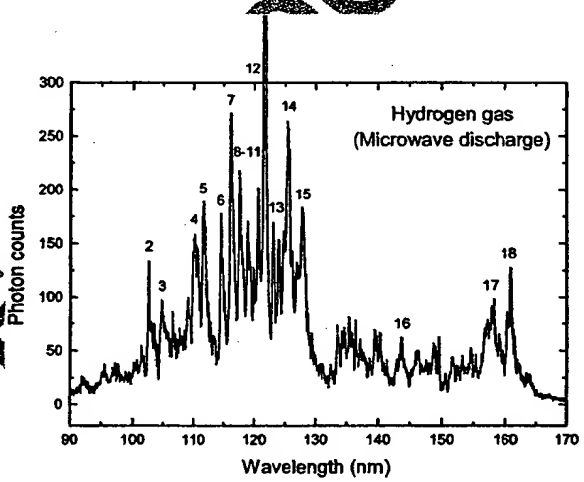

Fig. 7. Standard microwave discharge emission spectrum of hydrogen (900–1700 Å) recorded on the McPherson model 302 (Seya-Namioka type) EUV spectrometer.

5. Results

The standard hydrogen emission spectrum (850 and 1750 Å) obtained from a microwave plasma of hydrogen with a standard numbering order used in this analysis is shown in Fig. 7. The standard hydrogen spectrum was recorded by BlackLight Power Inc. using a photomultiplier tube detector. The EUV emission lines from hydrogen–KI plasmas produced by a hollow cathode discharge were recorded and identified on photographic films by INP Greifswald, Germany [25]. In order to make the wavelength assignments, all of the films were scanned, and the bitmap files were read out as shown in Figs. 8–12. Emission lines vs. scratches or other artifacts were determined from the films, and the wavelength assignments were based on the bitmap files shown in Figs. 8–12. A summary of the wavelength assignments and wavelength assignments based on the corrected calculated dispersion function are given in Table 5. Figs. 8–12 shows the observed spectral lines that are numbered on the respective numbered films as given in Table 5. Spectra were observed in the range around 100 nm only when KI was present; otherwise, no lines were observed on the films. In addition, the discharge current and a special positioning of

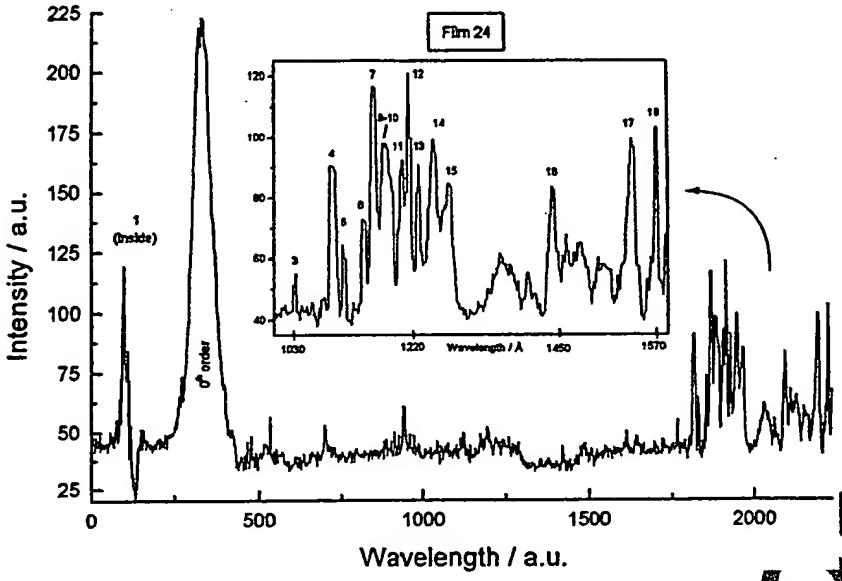

Fig. 8. The intensity of the scanned film 24 and the identified spectral lines recorded on the LSP-VUV 1-3S-M portable EUV grazing incidence spectrometer.

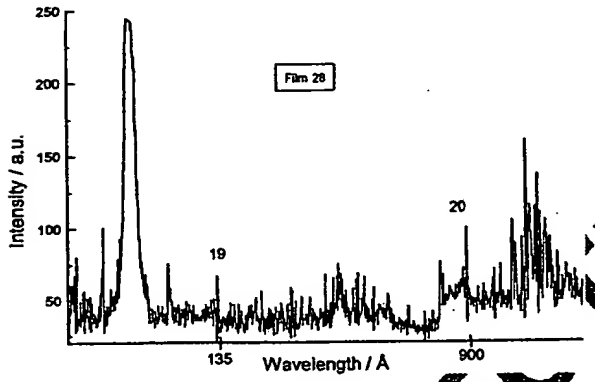

Fig. 9. The intensity of the scanned film 28 and the identified spectral lines recorded on the LSP-VUV 1-3S-M portable EUV grazing incidence spectrometer.

the sufficiently heated KI reservoir relative to the powered hollow cathode seem to be essential. The exact positions of the spectral lines were identified by using the Lyman-alpha line of hydrogen as a reference. The spectra comprised narrow and wide lines.

The wavelengths of the standard hydrogen peaks and the experimental peaks numbered 4–18 are given in Table 6. These experimental peaks match closely the wavelengths and intensities of the standard atomic and molecular hydrogen peaks. However, the identification of peaks 2 and 3 was problematic. It is known from the standard hydrogen spectrum that the most intense peak in the wavelength region between 102 and 105 nm is the hydrogen Lyman beta line located at 102.6 nm as shown in Fig. 7. If peak 2 shown in Fig. 11 is the Lyman beta line, then the experimental peak 3 shown Figs. 8 and 11 are different from the control since the peak 3 is the most intense peak in the region rather than the Lyman beta. Peak 3 could be assigned to $H^-(n = 1/4)$ at 11.2 eV as given in Table 7.

EUV lines not assignable to potassium, iodine, or hydrogen were observed at 73.0, 132.6, 513.6, 677.8, 885.9, and 1032.2 Å. The lines could be assigned to transitions of hydrino atoms and the emission from the excitation of the corresponding hydrino hydride ions. The assignments are given in Table 7.

The line at 73 Å which appeared as an inside-order-line was reproducible and was probably real. But, it had to be questioned, because of the observation of bunching into the sagittal direction and interference patterns into the meridional direction. This line was produced by the grating and was not subject to reflections as were some "ghosts" appearing as "absorption-lines" independently of the grating rulings. This "inside-order-line" vanished, when gratings with double or quadruple rulings were used. It cannot be excluded, that stimulated emission at this wavelength occurred from the hydrogen–KI plasma inside the hollow cathode or the area in front of it. According to the characteristics of the grating, the true wavelength could also be one-half, one-third, or less likely one-forth of 73 Å. It must be regarded as belonging to the regular emission of EUV light of the BLP plasma source.

By measuring the distances between the spectral lines on the printed scans and comparing it to those on the films, the average error in the calculation of the assigned wavelengths was determined to be about 30 Å in the region above 800 Å. Line 12 was determined to be the Lyman alpha

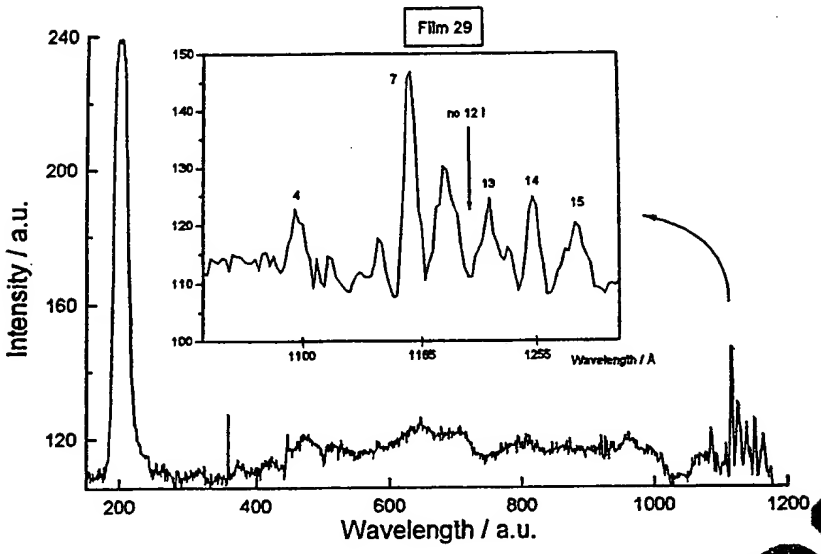

Fig. 10. The intensity of the scanned film 29 and the identified spectral lines recorded on the LSP-VUV 1-3S-M portable EUV grazing incidence spectrometer.

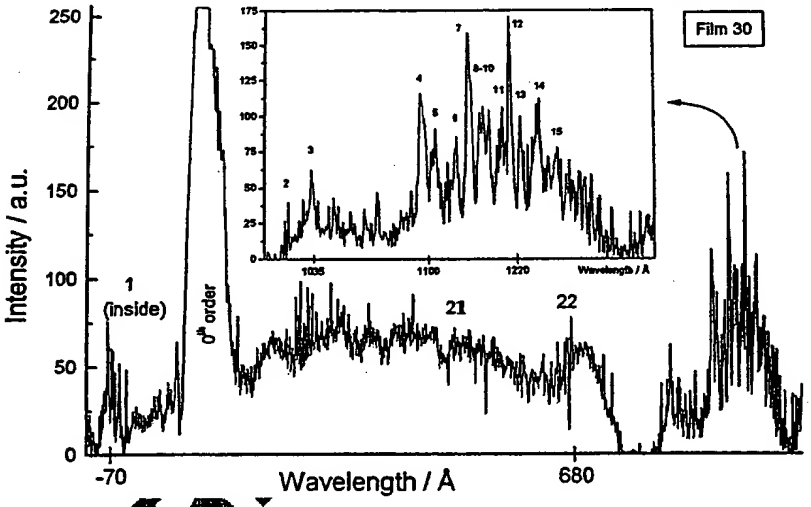

Fig. 11. The intensity of the scanned film 30 and the identified spectral lines recorded on the LSP-VUV 1-3S-M portable EUV grazing incidence spectrometer.

line of hydrogen (λ = 1215.7 Å) by comparing the structure of lines 3–15 with the known spectrum of hydrogen. This line was used to recalculate the dispersion function of grating #3. The error in the corrected data was about ±3 Å.

6. Discussion

The results support that potassium atoms reacted with atomic hydrogen to form novel hydrogen energy states. Potassium iodide present in the discharge of hydrogen served as a source of potassium metal which was observed to collect on the walls of the cell during operation. According to Eqs. (5)–(7), potassium metal reacts with atomic hydrogen present in the discharge and forms the hydrino atom H[a_H/4]. The energy released was expected to undergo *internal conversion* to increase the brightness of the plasma discharge since this is the common mechanism of relaxation. This is consistent with observation.

The product, H[a_H/4] may serve as a catalyst to form H[a_H/5] according to Eqs. (11)–(13). The transition of H[a_H/4] to H[a_H/5] induced by a resonance transfer of 27.21 eV, $m = 1$ in Eq. (3) with a metastable state excited

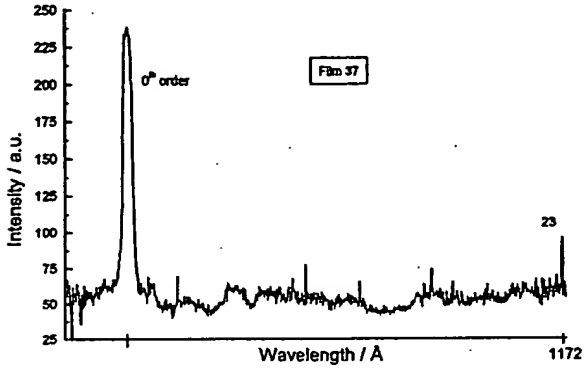

Fig. 12. The intensity of the scanned film 37 and the identified spectral lines recorded on the LSP-VUV 1-3S-M portable EUV grazing incidence spectrometer.

in $H[a_H/4]$ is represented by

$$27.2\text{ eV} + H\left[\frac{a_H}{4}\right] + H\left[\frac{a_H}{4}\right] \rightarrow H*\left[\frac{a_H}{4}\right] + H\left[\frac{a_H}{5}\right] + 27.2\text{ eV} + 95.2\text{ eV}, \quad (18)$$

$$H*\left[\frac{a_H}{4}\right] \rightarrow H\left[\frac{a_H}{4}\right] + 27.2\text{ eV}, \quad (19)$$

$$H\left[\frac{a_H}{4}\right] \rightarrow H\left[\frac{a_H}{5}\right] + 95.2\text{ eV} + 27.2\text{ eV}. \quad (20)$$

The energy emitted by a hydrino which has nonradiatively transferred $m \times 27.2$ eV of energy to a second hydrino may be emitted as a spectral line. Hydrinos may only accept energy by a nonradiative mechanism [18]; thus, rather than suppressing the emission through internal conversion they do not interact with the emitted radiation. The predicted 95.2 eV (130.3 Å) photon (peak # 19) shown in Fig. 9 is a close match with the observed 132.6 Å line. In Fig. 9, an additional peak (peak #20) was observed at 885.9 Å. It is proposed that peak #20 arises from inelastic hydrogen scattering of the metastable state $H*[a_H/4]$ formed by the resonant nonradiative energy transfer of 27.2 eV from a first $H[a_H/4]$ atom to a second as shown in Eq. (18). The metastable state then nonradiatively transfers part of the 27.2 eV excitation energy to excite atomic hydrogen initially in the state $1s^2S_{1/2}$ to the state $6h^2H_{11/2}$. This leaves a 13.98 eV (887.2 Å) photon, peak 20. The initial and final states for all hydrogen species and emitted photons are determined by the selection rule for conservation of angular momentum where the 13.98 eV photon corresponds to $m_\ell = 0$ and the initial and final states for the hydrino atom catalysts correspond to $m_\ell = -1$ and -2, respectively. In the case that the 95.2 eV (130.3 Å) photon (peak # 19) corresponds to $m_\ell = -1$, then angular momentum is conserved. The excited state hydrogen may then emit hydrogen lines that are observed in Fig. 9. Thus, the inelastic hydrogen scattering of the deexcitation of $H*[a_H/4]$ may be

Table 5
Wavelength assignments of identified emission peaks

Line no.	Average distance to zeroth order/mm on film no. #	Angle β/deg measured to zeroth order (grating #3[illegible])	λ/Å (entrance angle $\alpha = 4°$	λ/Å (recalculated entrance angle with $\alpha = 3.56°$)	Comments
1 (inside)	−5.21/Ø	1.62	80	73.0	
2	35.9/#30	11.1[illegible]	1070	1021.0	
3	36.2/#30	[illegible].18	1081.9	1032.9	
4	37.5/#30	11.[illegible]	1148.5	1095.8	Wide
5	37.8/#30	[illegible].72	1165.5	1114.4	
6	38.4/#30	[illegible]	1195.7	1143.7	
7	38.8/#30	12.03	1215	1162.1	Wide
8	39.1/#30	12.12	1229.6	1176.5	
9	39.2/#30	12.15	1234.3	1181.3	
10	39.3/#30	12.18	1239	1186.0	
11	39.7/#30	12.30	1258.8	1204.8	
12	39.9/#30	12.37	1270.3	1215.7	Strong, L_α
13	40.2/#30	12.46	1284.9	1230.8	
14	40.7/#30	12.61	1309.9	1254.7	
15	41.2/#30	12.76	1335	1279.2	
16	[illegible]/#30	13.74	1503	1443.7	
17	46.26/#24	14.30	1605.4	1541.9	Wide
18	46.78/#24	14.46	1633.7	1570.5	Wide
19	8.57/#28	2.66	144.1	132.6	Weak
20	32.68/#28	10.15	930.5	885.9	Weak
21	22.9/#30	7.12	544.8	513.6	Weak
22	27.5/#30	8.55	715.5	677.8	Weak
23	40.28/#37	12.09	1224	1171.8	

Table 6
Experimental peaks that matched the control hydrogen spectrum and are assigned to atomic and molecular hydrogen peaks

Peak number	Control hydrogen (Å)	Experimental (Å)
2	1025.4	1021.0
3	1047.0	—
4	1101.4	1095.8
5	1116.2	1114.4
6	1144.8	1143.7
7	1160.6	1162.1
8	1174.9	1176.5
9	1188.4	1181.3
10	1198.6	1186.0
11	1205.8	1204.8
12	1215.7	1215.7
13	1229.6	1230.8
14	1253.4	1254.7
15	1277.8	1279.2
16	1436.2	1443.7
17	1577.9	1541.9
18	1607.9	1570.5
23	Same as peak 8	1171.8

represented by

$$H * \left[\frac{a_H}{4}\right](m_\ell = 3) + H(n = 1; m_\ell = 0) \rightarrow$$
$$H\left[\frac{a_H}{4}\right](m_\ell = -2) + H(n = 6; m_\ell = 5)$$
$$+13.98\ \text{eV}(m_\ell = 0). \quad (21)$$

The product of the catalysis of atomic hydrogen with potassium metal, $H[a_H/4]$ may serve as both a catalyst and a reactant to form $H[a_H/3]$ and $H[a_H/6]$ according to Eq. (14). The transition of $H[a_H/4]$ to $H[a_H/6]$ induced by a multipole resonance transfer of 54.4 eV, $m = 2$ (Eq. (4)) and a transfer of 40.8 eV with a resonance state of $H[a_H/3]$ excited in $H[a_H/4]$ is represented by

$$H\left[\frac{a_H}{4}\right] + H\left[\frac{a_H}{4}\right] \rightarrow H\left[\frac{a_H}{6}\right] + H\left[\frac{a_H}{3}\right] + 176.8\ \text{eV}. \quad (22)$$

The predicted 176.8 eV (70.2 Å) photon is a close match with the observed 73.0 Å line.

The hydrinos are predicted to form hydrino hydride ions. A novel inorganic hydride compound KHI which comprises high binding energy hydride ions was synthesized by reaction of atomic hydrogen with potassium metal and potassium iodide [7]. The X-ray photoelectron spectroscopy (XPS) spectrum of KHI differed from that of KI by having additional peaks at 9.1 and 11.1 eV. The XPS peaks centered at 9.1 and 11.1 eV that do not correspond to any other primary element peaks may correspond to the $H^-(n = 1/4)$ $E_b = 11.2$ eV hydride ion predicted by Mills [18] (Eq. (16)) in two different chemical environments where E_b is the predicted vacuum binding energy. In this case, the reaction to form $H^-(n = 1/4)$ is given by Eqs. (5)–(7) and (15). Hydrino hydride ions $H^-(n = 1/4)$, $H^-(n = 1/5)$, and $H^-(n = 1/6)$ corresponding to the corresponding hydrino atoms were anticipated. The predicted energy of emission due to these ions in the plasma discharge was anticipated to be higher than that given in Table 1 due to the formation of stable compounds such as KHI comprising these ions. Emission peaks which could not be assigned to hydrogen, potassium, or iodine were observed at 1032.9 Å (12.0 eV), 677.8 Å (18.3 eV), and 513.6 Å (24.1 eV). The binding energies of hydrino hydride ions $H^-(n = 1/4)$, $H^-(n = 1/5)$, and $H^-(n = 1/6)$ corresponding to the corresponding hydrino atoms are 11.23, 16.7, and 22.81 eV. The emissions were 1–2 eV higher than predicted which may be due to the presence of these ions in compounds with chemical environments different from that of vacuum. The excitation was due to the plasma electron bombardment. Additional studies are in progress to collect the compounds formed in the reaction chamber so that XPS may be performed and the XPS spectrum may be compared with the EUV peaks.

7. Conclusion

Lines which could be assigned to all of the hydrino transitions and hydrino hydride ions possible in the spectral range of 2.5–180 nm starting with a potassium catalyst (Eqs. (5)–(7)) were observed. Intense EUV emission was observed from atomic hydrogen in the presence of potassium which ionizes at integer multiples of the potential energy of atomic hydrogen (Eq. (3)). The release of energy from hydrogen as evidenced by the EUV emission must result in a lower-energy state of hydrogen. The data supports that potassium metal reacts with atomic hydrogen present in the discharge and forms the hydrino atom $H[a_H/4]$. The energy released undergoes *internal conversion* to increase the brightness of the plasma discharge. The product, $H[a_H/4]$ serves as both a catalyst and a reactant to form $H[a_H/5]$ with a 132.6 Å and 885.9 Å emission and $H[a_H/6]$ with a 73.0 Å emission according to Eqs. (18)–(21) and (22), respectively. Hydrino hydride ions $H^-(n=1/4)$, $H^-(n=1/5)$, and $H^-(n = 1/6)$ corresponding to the hydrino atoms of the same quantum state were formed in the plasma as evidenced by the emissions at 513.6, 677.8, and 1032.9 Å, respectively. The emissions were 1–2 eV higher than predicted which may be due to the presence of these ions in compounds with chemical environments different from that of vacuum. Novel compounds containing hydrino hydride ions have been isolated as products of the reaction of atomic hydrogen with potassium atoms and ions [6–12] identified as catalysts in a recent EUV study [1–4]. The formation of novel compounds based on hydrino atoms is substantial evidence supporting catalysis of hydrogen as the mechanism of the observed EUV emission.

J. J. Balmer showed in 1885 that the frequencies for some of the lines observed in the emission spectrum of atomic hydrogen could be expressed with a completely empirical

Table 7
Observed emission data from hydrogen–KI plasmas produced by a hollow cathode discharge that cannot be assigned to atomic or molecular hydrogen

Peak	#	Observed		Peak assignment	Predicted	
		Wavelength (Å)	Energy (eV)		Energy (eV)	Wavelength (Å)
1	(inside)	73.0	169.9	1/4 → 1/6 H transition[a]	176.8	70.2
3	(#30)	1032.9	12.0	$H^-(1/4)$[b,c]	11.23	1104
19	(#28)	132.6	93.5	1/4 → 1/5 H transition[d]	95.2	130.3
20	(#28)	885.9	14.0	Inelastic H scattering of $H*\left[\frac{a_H}{4}\right]$[e]	13.98	887.2
21	(#30)	513.6	24.15	$H^-(1/6)$[c]	22.8	543
22	(#30)	677.8	18.30	$H^-(1/5)$[c]	16.7	742

[a]Transition induced by a resonance state excited in $H[a_H/4]$

$$H\left[\frac{a_H}{4}\right]+H\left[\frac{a_H}{4}\right]\rightarrow H\left[\frac{a_H}{6}\right]+H\left[\frac{a_H}{3}\right]+176.8\ \text{eV}$$

[b]I^+ has a peak at 1034.66 Å, [31] but none of the other iodine lines were detected including much stronger lines
[c]The hydride ion emission is anticipated to be shift to shorter wavelengths due to its presence in a chemical compound
[d]Transition induced by a metastable state excited in $H[a_H/4]$

$$27.2\ \text{eV}+H\left[\frac{a_H}{4}\right]+H\left[\frac{a_H}{4}\right]\rightarrow H*\left[\frac{a_H}{4}\right]+H\left[\frac{a_H}{5}\right]+27.2\ \text{eV}+95.2\ \text{eV},$$

$$H*\left[\frac{a_H}{4}\right]\rightarrow H\left[\frac{a_H}{4}\right]+27.2\ \text{eV},$$

$$H\left[\frac{a_H}{4}\right]\rightarrow H\left[\frac{a_H}{5}\right]+95.2\ \text{eV}+27.2\ \text{eV}.$$

[e]Hydrogen inelastic scattered peak of $H*[a_H/4]$ deexcitation

$$H*\left[\frac{a_H}{4}\right]+H(n=1;m_\ell=0)\rightarrow H\left[\frac{a_H}{4}\right]+H(n=6;m_\ell=5)+13.98\ \text{eV}$$

relationship. This approach was later extended by J. R. Rydberg, who showed that all of the spectral lines of atomic hydrogen were given by the equation

$$\bar{\nu}=R\left(\frac{1}{n_f^2}-\frac{1}{n_i^2}\right), \tag{23}$$

where $R=109{,}677\ \text{cm}^{-1}$, $n_f=1,2,3,\ldots$, $n_i=2,3,4,\ldots$, and $n_i>n_f$.

Niels Bohr, in 1913, developed a theory for atomic hydrogen that gave energy levels in agreement with Rydberg's equation. An identical equation, based on a totally different theory for the hydrogen atom, was developed by E. Schrödinger and independently by W. Heisenberg, in 1926:

$$E_n=-\frac{e^2}{n^2 8\pi\varepsilon_0 a_H}=-\frac{13.598\ \text{eV}}{n^2}, \tag{24a}$$

$$n=1,2,3\ldots, \tag{24b}$$

where a_H is the Bohr radius for the hydrogen atom (52.947 pm), e is the magnitude of the charge of the electron, and ε_0 is the vacuum permittivity. The EUV emission of atomic hydrogen with a source of potassium indicates that Eq. (24b), should be replaced by Eq. (24c),

$$n=1,2,3,\ldots,\ \text{and},\ n=\tfrac{1}{2},\tfrac{1}{3},\tfrac{1}{4},\ldots\ . \tag{24c}$$

A number of independent experimental observations also lead to the conclusion that atomic hydrogen can exist in fractional quantum states that are at lower energies than the traditional "ground" ($n=1$) state. The detection of atomic hydrogen in fractional quantum energy levels below the traditional "ground" state — hydrinos — was reported [18,30] by the assignment of soft X-ray emissions from the interstellar medium, the Sun, and stellar flares, and by assignment of certain lines obtained by the far-infrared absolute spectrometer (FIRAS) on the Cosmic Background Explorer. The assigned hydrogen transition reactions were similar to those shown in Table 7. The detection of a new molecular species — the diatomic hydrino molecule — was reported by the assignment of certain infrared line emissions from the Sun. The detection of a new hydride species — hydrino hydride ion — was reported by the assignment of certain soft

X-ray, ultraviolet (UV), and visible emissions from the Sun. This has implications for several unresolved astrophysical problems such as the Solar neutrino paradox and the identity of dark matter. The present study also has the important technological implications of the discovery of a new energy source and a new field of hydrogen chemistry.

Acknowledgements

Special thanks to J. Conrads, S. Goetze, J. Schwartz, and H. Lange for performing the experiments and for identifying spectral lines to be assigned, to Ying Lu for reviewing the data and making the assignments to known transitions where possible, and J. Conrads for reviewing this manuscript and providing helpful comments.

References

[1] Mills R, Dong J, Lu Y. Observation of extreme ultraviolet hydrogen emission from incandescently heated hydrogen gas with certain catalysts. 1999 Pacific Conference on Chemistry and Spectroscopy and the 35th ACS Western Regional Meeting, Ontario Convention Center, California, October 6–8, 1999.

[2] Mills R, Dong J, Lu Y. Observation of extreme ultraviolet hydrogen emission from incandescently heated hydrogen gas with certain catalysts. Int J Hydrogen Energy 2000;25: 919–43.

[3] Mills R. Temporal behavior of light-emission in the visible spectral range from a Ti-K2CO3-H-Cell. Int J Hydrogen Energy, in press.

[4] Mills R, Lu Y, Onuma T. Formation of a hydrogen plasma from an incandescently heated hydrogen–potassium gas mixture and plasma decay upon removal of heater power. Int J Hydrogen Energy, in press.

[5] Mills R, Nansteel M, Lu Y. Observation of extreme ultraviolet hydrogen emission from incandescently heated hydrogen gas with strontium that produced an anomalous optically measured power balance. Int J Hydrogen Energy, in press.

[6] Mills R, Dhandapani B, Greenig N, He J, Dong J, Lu Y, Conrads H. Formation of an energetic plasma and novel hydrides from incandescently heated hydrogen gas with certain catalysts, June ACS Meeting, 29th Northeast Regional Meeting, University of Connecticut, Storrs, CT, June 18–21, 2000.

[7] Mills R, Dhandapani B, Greenig N, He J. Synthesis and characterization of potassium iodo hydride. Int J Hydrogen Energy, in press.

[8] Mills R. Novel inorganic hydride. Int J Hydrogen Energy 2000;25:669–83.

[9] Mills R. Novel hydrogen compounds from a potassium carbonate electrolytic cell. Fusion Technol 2000;37(2):157–82.

[10] Mills R, He J, Dhandapani B. Novel hydrogen compounds. 1999 Pacific Conference on Chemistry and Spectroscopy and the 35th ACS Western Regional Meeting, Ontario Convention Center, California, October 6–8, 1999.

[11] Mills R, Dhandapani B, Nansteel M, He J. Synthesis and characterization of novel hydride compounds. Int J Hydrogen Energy, in press.

[12] Mills R. Highly stable novel inorganic hydrides. J Mater Res., submitted for publication.

[13] Phillips JH. Guide to the sun, Cambridge, Great Britain: Cambridge University Press, 1992. p. 16–20.

[14] Sampson JAR. Techniques of vacuum ultraviolet spectroscopy. Pied Publications, 1980. p. 94–179.

[15] Sci News, 12/6/97, p. 366.

[16] Fujimoto T, Sawada K, Takahata K. J Appl Phys 1989;66(6):2315–9.

[17] Hollander A, Wertheimer MR. J Vac Sci Technol A 1994;12(3):879–82.

[18] Mills R. The grand unified theory of classical quantum mechanics, January 2000 Edition, BlackLight Power, Inc., Cranbury, New Jersey, Distributed by Amazon.com.

[19] Sidgwick NV. The chemical elements and their compounds, vol. I. Oxford: Clarendon Press, 1950. p. 17.

[20] Lamb MD. Luminescence spectroscopy. London: Academic Press, 1978. p. 93.

[21] Linde DR. CRC handbook of chemistry and physics, 79th ed. Boca Raton, FL: CRC Press, 1998–9. p. 10-175–7.

[22] Thompson BJ. Handbook of nonlinear optics. New York: Marcel Dekker, Inc., 1996. p. 497–548.

[23] Shen YR. The principles of nonlinear optics. New York: Wiley, 1984. p. 203–10.

[24] de Beauvoir B, Nez F, Julien L, Cagnac B, Biraben F, Touahri D, Hilico L, Acef O, Clairon A, Zondy JJ. Phys Rev Lett 1997;78(3):440–3.

[25] Conrads JPF, Goetze S, Schwartz J, Lange H. Investigation of hydrogen–KI plasmas produced by a hollow cathode discharge. December 18, 1998, Institut fur Niedertemperatur-Plasmaphysik e.V., Friedrich-Ludwig-Jahn-Strasse 19, 17489 Greifswald, Germany.

[26] Bogen P, Conrads H, Gatti G, Kohlhaas W. JOSA 1968;58(3):203–6.

[27] Rocca JJ, Marconi MC, Tomasel FG. J Quant Electron 1983;29:180.

[28] Kunze HJ, Koshelev KN, Steden C, Uskov D, Wiesebrink HT. Phys Rev A 1993;193:183.

[29] Conrads JPF Institut fur Niedertemperatur-Plasmaphysik e.V., personal communication.

[30] Mills R. The hydrogen atom revisited. Int J Hydrogen Energy, in press.

[31] NIST Atomic Spectra Database, www.physics.nist.gov/cgibin/AtData/display.ksh.